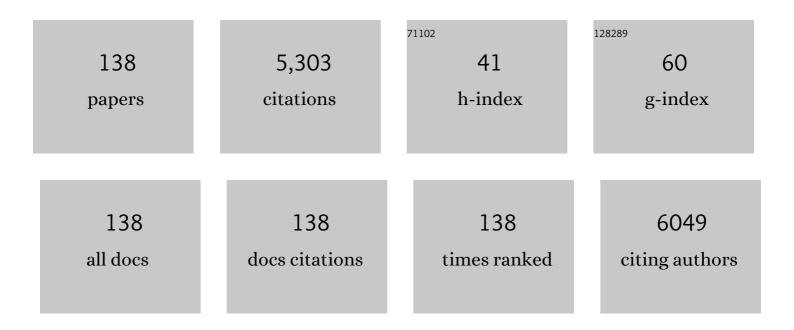
List of Publications by Year in descending order

Source: https://exaly.com/author-pdf/8045430/publications.pdf Version: 2024-02-01



ZHICANC XII

#	Article	IF	CITATIONS
1	Bioresponsive immune-booster-based prodrug nanogel for cancer immunotherapy. Acta Pharmaceutica Sinica B, 2022, 12, 451-466.	12.0	66
2	Applying nanotechnology to boost cancer immunotherapy by promoting immunogenic cell death. Chinese Chemical Letters, 2022, 33, 1718-1728.	9.0	42
3	Acidic TMEâ€Responsive Nanoâ€Bi <sub>2</sub> Se <sub>3</sub> @MnCaP as a NIRâ€IIâ€Triggered Free Radical Generator for Hypoxiaâ€Irrelevant Phototherapy with High Specificity and Immunogenicity. Small, 2022, 18, e2104302.	10.0	19
4	Silk fibroin-capped metal-organic framework for tumor-specific redox dyshomeostasis treatment synergized by deoxygenation-driven chemotherapy. Acta Biomaterialia, 2022, 138, 545-560.	8.3	18
5	MIL-47(V) catalytic conversion of H2O2 for sensitive H2O2 detection and tumor cell inhibition. Sensors and Actuators B: Chemical, 2022, 354, 131201.	7.8	19
6	Study on the stability and oral bioavailability of curcumin loaded (-)-epigallocatechin-3-gallate/poly(N-vinylpyrrolidone) nanoparticles based on hydrogen bonding-driven self-assembly. Food Chemistry, 2022, 378, 132091.	8.2	18
7	Engineered nanogels simultaneously implement HDAC inhibition and chemotherapy to boost antitumor immunity via pyroptosis. Applied Materials Today, 2022, 26, 101363.	4.3	9
8	Microenvironment-responsive chemotherapeutic nanogels for enhancing tumor therapy via DNA damage and glutathione consumption. Chinese Chemical Letters, 2022, 33, 4197-4202.	9.0	20
9	Bimetallic PdPt-based nanocatalysts for Photothermal-Augmented tumor starvation and sonodynamic therapy in NIR-II biowindow assisted by an oxygen Self-Supply strategy. Chemical Engineering Journal, 2022, 435, 135085.	12.7	30
10	Engineering prodrug nanomicelles as pyroptosis inducer for codelivery of PI3K/mTOR and CDK inhibitors to enhance antitumor immunity. Acta Pharmaceutica Sinica B, 2022, 12, 3139-3155.	12.0	13
11	Bioresponsive nanotherapy for preventing dental caries by inhibiting multispecies cariogenic biofilms. Bioactive Materials, 2022, 14, 1-14.	15.6	27
12	Inspired heat shock protein alleviating prodrug enforces immunogenic photodynamic therapy by eliciting pyroptosis. Nano Research, 2022, 15, 3398-3408.	10.4	17
13	The Systematic Evaluation of Physicochemical and Biological Properties In Vitro and In Vivo for Natural Silk Fibroin Nanoparticles. Advanced Fiber Materials, 2022, 4, 1141-1152.	16.1	9
14	A platinum nanourchin-based multi-enzymatic platform to disrupt mitochondrial function assisted by modulating the intracellular H2O2 homeostasis. Biomaterials, 2022, 286, 121572.	11.4	15
15	Active targeting redox-responsive mannosylated prodrug nanocolloids promote tumor recognition and cell internalization for enhanced colon cancer chemotherapy. Acta Biomaterialia, 2022, 147, 299-313.	8.3	20
16	Bioengineered nanogels for cancer immunotherapy. Chemical Society Reviews, 2022, 51, 5136-5174.	38.1	81
17	Bioresponsive prodrug nanogel-based polycondensate strategy deepens tumor penetration and potentiates oxidative stress. Chemical Engineering Journal, 2021, 420, 127657.	12.7	35
18	Facile engineering of silk fibroin capped AuPt bimetallic nanozyme responsive to tumor microenvironmental factors for enhanced nanocatalytic therapy. Theranostics, 2021, 11, 107-116.	10.0	25

#	Article	IF	CITATIONS
19	Polydopamine (PDA)-activated cobalt sulfide nanospheres responsive to tumor microenvironment (TME) for chemotherapeutic-enhanced photothermal therapy. Chinese Chemical Letters, 2021, 32, 1055-1060.	9.0	34
20	Multiâ€Responsive Bottlebrush‣ike Unimolecules Selfâ€Assembled Nanoâ€Riceball for Synergistic Sonoâ€Chemotherapy. Small Methods, 2021, 5, e2000416.	8.6	47
21	ROS-responsive cyclodextrin nanoplatform for combined photodynamic therapy and chemotherapy of cancer. Chinese Chemical Letters, 2021, 32, 162-167.	9.0	98
22	Intradermal administration of green synthesized nanosilver (NS) through film-coated PEGDA microneedles for potential antibacterial applications. Biomaterials Science, 2021, 9, 2244-2254.	5.4	21
23	Reduction-Responsive Chemo-Capsule-Based Prodrug Nanogel for Synergistic Treatment of Tumor Chemotherapy. ACS Applied Materials & Interfaces, 2021, 13, 8940-8951.	8.0	35
24	Silk Sericin-Based Nanoparticle as the Photosensitizer Chlorin e6 Carrier for Enhanced Cancer Photodynamic Therapy. ACS Sustainable Chemistry and Engineering, 2021, 9, 3213-3222.	6.7	7
25	Inspired Epigenetic Modulation Synergy with Adenosine Inhibition Elicits Pyroptosis and Potentiates Cancer Immunotherapy. Advanced Functional Materials, 2021, 31, 2100007.	14.9	39
26	Engineering silk sericin decorated zeolitic imidazolate framework-8 nanoplatform to enhance chemotherapy. Colloids and Surfaces B: Biointerfaces, 2021, 200, 111594.	5.0	16
27	GSH/pH dual-responsive and HA-targeting nano-carriers for effective drug delivery and controlled release. Journal of Drug Delivery Science and Technology, 2021, 62, 102327.	3.0	9
28	Supramolecular Tadalafil Nanovaccine for Cancer Immunotherapy by Alleviating Myeloidâ€Đerived Suppressor Cells and Heightening Immunogenicity. Small Methods, 2021, 5, e2100115.	8.6	44
29	Engineering oxygen-deficient ZrO2-x nanoplatform as therapy-activated "immunogenic cell death (ICD)―inducer to synergize photothermal-augmented sonodynamic tumor elimination in NIR-II biological window. Biomaterials, 2021, 272, 120787.	11.4	77
30	A thiol-responsive and self-immolative podophyllotoxin prodrug for cancer therapy. Tetrahedron Letters, 2021, 71, 153044.	1.4	6
31	Promotion of the anticancer activity of curcumin based on a metal–polyphenol networks delivery system. International Journal of Pharmaceutics, 2021, 602, 120650.	5.2	18
32	Catalytically Active CoFe <sub>2</sub> O <sub>4</sub> Nanoflowers for Augmented Sonodynamic and Chemodynamic Combination Therapy with Elicitation of Robust Immune Response. ACS Nano, 2021, 15, 11953-11969.	14.6	114
33	Acid-Sensitive Supramolecular Nanoassemblies with Multivalent Interaction: Effective Tumor Retention and Deep Intratumor Infiltration. ACS Applied Materials & Interfaces, 2021, 13, 37680-37692.	8.0	18
34	Tumor microenvironment responsive biomimetic copper peroxide nanoreactors for drug delivery and enhanced chemodynamic therapy. Chemical Engineering Journal, 2021, 416, 129037.	12.7	53
35	Cylindrical polymer brushes-anisotropic unimolecular micelle drug delivery system for enhancing the effectiveness of chemotherapy. Bioactive Materials, 2021, 6, 2894-2904.	15.6	48
36	Near-infrared light-triggered synergistic antitumor therapy based on hollow ZIF-67-derived Co3S4-indocyanine green nanocomplex as a superior reactive oxygen species generator. Materials Science and Engineering C, 2021, 130, 112465.	7.3	10

#	Article	IF	CITATIONS
37	Multifunctional SGQDs-CORM@HA nanosheets for bacterial eradication through cascade-activated "nanoknife―effect and photodynamic/CO gas therapy. Biomaterials, 2021, 277, 121084.	11.4	30
38	Iron-based nanoparticles for MR imaging-guided ferroptosis in combination with photodynamic therapy to enhance cancer treatment. Nanoscale, 2021, 13, 4855-4870.	5.6	88
39	MnO <sub>2</sub> -capped silk fibroin (SF) nanoparticles with chlorin e6 (Ce6) encapsulation for augmented photo-driven therapy by modulating the tumor microenvironment. Journal of Materials Chemistry B, 2021, 9, 3677-3688.	5.8	10
40	Polyamino acid calcified nanohybrids induce immunogenic cell death for augmented chemotherapy and chemo-photodynamic synergistic therapy. Theranostics, 2021, 11, 9652-9666.	10.0	15
41	Ultrasound (US)-activated redox dyshomeostasis therapy reinforced by immunogenic cell death (ICD) through a mitochondrial targeting liposomal nanosystem. Theranostics, 2021, 11, 9470-9491.	10.0	29
42	Microenvironmentâ€Responsive Prodrugâ€Induced Pyroptosis Boosts Cancer Immunotherapy. Advanced Science, 2021, 8, e2101840.	11.2	160
43	Acidic microenvironment responsive polymeric MOF-based nanoparticles induce immunogenic cell death for combined cancer therapy. Journal of Nanobiotechnology, 2021, 19, 455.	9.1	15
44	The design and synthesis of dextran-doxorubicin prodrug-based pH-sensitive drug delivery system for improving chemotherapy efficacy. Asian Journal of Pharmaceutical Sciences, 2020, 15, 605-616.	9.1	38
45	Responsive agarose hydrogel incorporated with natural humic acid and MnO <sub>2</sub> nanoparticles for effective relief of tumor hypoxia and enhanced photo-induced tumor therapy. Biomaterials Science, 2020, 8, 353-369.	5.4	53
46	Light-activated oxygen self-supplied starving therapy in near-infrared (NIR) window and adjuvant hyperthermia-induced tumor ablation with an augmented sensitivity. Biomaterials, 2020, 234, 119771.	11.4	59
47	A bottlebrush-architectured dextran polyprodrug as an acidity-responsive vector for enhanced chemotherapy efficiency. Biomaterials Science, 2020, 8, 473-484.	5.4	29
48	Reactive oxygen species-activatable camptothecin polyprodrug based dextran enhances chemotherapy efficacy by damaging mitochondria. Journal of Materials Chemistry B, 2020, 8, 1245-1255.	5.8	9
49	Rational design of oxygen deficient TiO <sub>2â<sup>~</sup>x</sub> nanoparticles conjugated with chlorin e6 (Ce6) for photoacoustic imaging-guided photothermal/photodynamic dual therapy of cancer. Nanoscale, 2020, 12, 1707-1718.	5.6	23
50	Facile synthesis of hollow mesoporous nickel sulfide nanoparticles for highly efficient combinatorial photothermal–chemotherapy of cancer. Journal of Materials Chemistry B, 2020, 8, 7766-7776.	5.8	15
51	Biomimetic CoO@AuPt nanozyme responsive to multiple tumor microenvironmental clues for augmenting chemodynamic therapy. Biomaterials, 2020, 257, 120279.	11.4	99
52	Glutathione-Responsive Multifunctional "Trojan Horse―Nanogel as a Nanotheranostic for Combined Chemotherapy and Photodynamic Anticancer Therapy. ACS Applied Materials & Interfaces, 2020, 12, 50896-50908.	8.0	37
53	The synthesis of two-dimensional Bi <sub>2</sub> Te <sub>3</sub> @SiO <sub>2</sub> core–shell nanosheets for fluorescence/photoacoustic/infrared (FL/PA/IR) tri-modal imaging-guided photothermal/photodynamic combination therapy. Biomaterials Science, 2020, 8, 5874-5887.	5.4	7
54	A HMCuS@MnO <sub>2</sub> nanocomplex responsive to multiple tumor environmental clues for photoacoustic/fluorescence/magnetic resonance trimodal imaging-guided and enhanced photothermal/photodynamic therapy. Nanoscale, 2020, 12, 12508-12521.	5.6	31

ZHIGANG XU

#	Article	IF	CITATIONS
55	Activatable Formation of Emissive Excimers for Highly Selective Detection of β-Galactosidase. Analytical Chemistry, 2020, 92, 5733-5740.	6.5	27
56	Polymeric micelles as delivery systems. , 2020, , 261-278.		1
57	Prodrugâ€Based Versatile Nanomedicine for Enhancing Cancer Immunotherapy by Increasing Immunogenic Cell Death. Small, 2020, 16, e2000214.	10.0	73
58	Boosting O <sub>2</sub> <sup>•â^'</sup> Photogeneration via Promoting Intersystemâ€Crossing and Electronâ€Donating Efficiency of Azaâ€BODIPYâ€Based Nanoplatforms for Hypoxicâ€Tumor Photodynamic Therapy. Small Methods, 2020, 4, 2000013.	8.6	89
59	A boron nitride electrode modified with a nanocomposite prepared from an ionic liquid and tungsten disulfide for voltammetric sensing of 4-aminophenol. Mikrochimica Acta, 2019, 186, 614.	5.0	16
60	Development and prospects of microfluidic platforms for sperm inspection. Analytical Methods, 2019, 11, 4547-4560.	2.7	6
61	Codelivery of doxorubicin and camptothecin by dual-responsive unimolecular micelle-based β-cyclodextrin for enhanced chemotherapy. Colloids and Surfaces B: Biointerfaces, 2019, 183, 110428.	5.0	27
62	Biomineralization-inspired Crystallization of Manganese Oxide on Silk Fibroin Nanoparticles for <i>in vivo</i> MR/fluorescence Imaging-assisted Tri-modal Therapy of Cancer. Theranostics, 2019, 9, 6314-6333.	10.0	67
63	Mitochondria-Specific Anticancer Drug Delivery Based on Reduction-Activated Polyprodrug for Enhancing the Therapeutic Effect of Breast Cancer Chemotherapy. ACS Applied Materials & Interfaces, 2019, 11, 29330-29340.	8.0	30
64	Novel Oxygen-Deficient Zirconia (ZrO <sub>2–<i>x</i></sub> ) for Fluorescence/Photoacoustic Imaging-Guided Photothermal/Photodynamic Therapy for Cancer. ACS Applied Materials & Interfaces, 2019, 11, 41127-41139.	8.0	35
65	Transdermal delivery of therapeutics through dissolvable gelatin/sucrose films coated on PEGDA microneedle arrays with improved skin permeability. Journal of Materials Chemistry B, 2019, 7, 7515-7524.	5.8	29
66	A Reductionâ€responsive Amphiphilic Methotrexateâ€Podophyllotoxin Conjugate for Targeted Chemotherapy. Chemistry - an Asian Journal, 2019, 14, 3840-3844.	3.3	19
67	Co-delivery of chlorin e6 and doxorubicin using PEGylated hollow nanocapsules for â€~all-in-one' tumor theranostics. Nanomedicine, 2019, 14, 2273-2292.	3.3	6
68	Smart Unimolecular Micelle-Based Polyprodrug with Dual-Redox Stimuli Response for Tumor Microenvironment: Enhanced in Vivo Delivery Efficiency and Tumor Penetration. ACS Applied Materials & Interfaces, 2019, 11, 36130-36140.	8.0	56
69	Construction of a Z-scheme g-C <sub>3</sub> N <sub>4</sub> /Ag/AgI heterojunction for highly selective photoelectrochemical detection of hydrogen sulfide. Chemical Communications, 2019, 55, 11940-11943.	4.1	43
70	Tumor-Microenvironment-Activatable Nanoreactor Based on a Polyprodrug for Multimodal-Imaging-Medicated Enhanced Cancer Chemo/Phototherapy. ACS Applied Materials & Interfaces, 2019, 11, 40704-40715.	8.0	29
71	Highly Porous Silk Fibroin Scaffold Packed in PEGDA/Sucrose Microneedles for Controllable Transdermal Drug Delivery. Biomacromolecules, 2019, 20, 1334-1345.	5.4	69
72	Rapid prototyping of Nanoroughened polydimethylsiloxane surfaces for the enhancement of immunomagnetic isolation and recovery of rare tumor cells. Biomedical Microdevices, 2019, 21, 58.	2.8	6

ZHIGANG XU

#	Article	IF	CITATIONS
73	Enhanced Tumor Penetration and Chemotherapy Efficiency by Covalent Self-Assembled Nanomicelle Responsive to Tumor Microenvironment. Biomacromolecules, 2019, 20, 2637-2648.	5.4	19
74	Stimuli responsive PEGylated bismuth selenide hollow nanocapsules for fluorescence/CT imaging and light-driven multimodal tumor therapy. Biomaterials Science, 2019, 7, 3025-3040.	5.4	24
75	Indocyanine green-modified hollow mesoporous Prussian blue nanoparticles loading doxorubicin for fluorescence-guided tri-modal combination therapy of cancer. Nanoscale, 2019, 11, 5717-5731.	5.6	64
76	PEGylated mesoporous Bi2S3 nanostars loaded with chlorin e6 and doxorubicin for fluorescence/CT imaging-guided multimodal therapy of cancer. Nanomedicine: Nanotechnology, Biology, and Medicine, 2019, 17, 1-12.	3.3	27
77	Starburst Diblock Polyprodrugs: Reduction-Responsive Unimolecular Micelles with High Drug Loading and Robust Micellar Stability for Programmed Delivery of Anticancer Drugs. Biomacromolecules, 2019, 20, 1190-1202.	5.4	44
78	Phase-Change Material Packaged within Hollow Copper Sulfide Nanoparticles Carrying Doxorubicin and Chlorin e6 for Fluorescence-Guided Trimodal Therapy of Cancer. ACS Applied Materials & Interfaces, 2019, 11, 417-429.	8.0	84
79	Facile Fabrication of Oxidation-Responsive Polymeric Nanoparticles for Effective Anticancer Drug Delivery. Molecular Pharmaceutics, 2019, 16, 49-59.	4.6	15
80	Oral Drug Delivery Systems for Ulcerative Colitis Therapy: A Comparative Study with Microparticles and Nanoparticles. Current Cancer Drug Targets, 2019, 19, 304-311.	1.6	14
81	Threeâ€dimensional microfluidic chip with twinâ€layer herringbone structure for high efficient tumor cell capture and release via antibodyâ€conjugated magnetic microbeads. Electrophoresis, 2018, 39, 1452-1459.	2.4	17
82	Water-soluble fluorescent unimolecular micelles: ultra-small size, tunable fluorescence emission from the visible to NIR region and enhanced biocompatibility for <i>in vitro</i> and <i>in vivo</i> bioimaging. Chemical Communications, 2018, 54, 6252-6255.	4.1	20
83	Reduction-active polymeric prodrug micelles based on α-cyclodextrin polyrotaxanes for triggered drug release and enhanced cancer therapy. Carbohydrate Polymers, 2018, 193, 153-162.	10.2	34
84	Polydopamineâ€collagen complex to enhance the biocompatibility of polydimethylsiloxane substrates for sustaining longâ€term culture of L929 fibroblasts and tendon stem cells. Journal of Biomedical Materials Research - Part A, 2018, 106, 408-418.	4.0	27
85	Acid-activatable doxorubicin prodrug micelles with folate-targeted and ultra-high drug loading features for efficient antitumor drug delivery. Journal of Materials Science, 2018, 53, 892-907.	3.7	11
86	PEGylated magnetic Prussian blue nanoparticles as a multifunctional therapeutic agent for combined targeted photothermal ablation and pH-triggered chemotherapy of tumour cells. Journal of Colloid and Interface Science, 2018, 509, 384-394.	9.4	34
87	PEGylated Polydopamine Nanoparticles Incorporated with Indocyanine Green and Doxorubicin for Magnetically Guided Multimodal Cancer Therapy Triggered by Near-Infrared Light. ACS Applied Nano Materials, 2018, 1, 325-336.	5.0	34
88	Reduction stimuli-responsive unimolecular polymeric prodrug based on amphiphilic dextran-framework for antitumor drug delivery. Carbohydrate Polymers, 2018, 182, 235-244.	10.2	42
89	A simple technique of constructing nano-roughened polydimethylsiloxane surface to enhance mesenchymal stem cell adhesion and proliferation. Microfluidics and Nanofluidics, 2018, 22, 1.	2.2	27
90	Acid-active supramolecular anticancer nanoparticles based on cyclodextrin polyrotaxanes damaging both mitochondria and nuclei of tumor cells. Biomaterials Science, 2018, 6, 3126-3138.	5.4	25

#	Article	IF	CITATIONS
91	Indocyanine Green-Conjugated Magnetic Prussian Blue Nanoparticles for Synchronous Photothermal/Photodynamic Tumor Therapy. Nano-Micro Letters, 2018, 10, 74.	27.0	81
92	Injectable and Natural Humic Acid/Agarose Hybrid Hydrogel for Localized Light-Driven Photothermal Ablation and Chemotherapy of Cancer. ACS Biomaterials Science and Engineering, 2018, 4, 4266-4277.	5.2	41
93	Calcium-carbonate packaging magnetic polydopamine nanoparticles loaded with indocyanine green for near-infrared induced photothermal/photodynamic therapy. Acta Biomaterialia, 2018, 81, 242-255.	8.3	53
94	PEGDA/PVP Microneedles with Tailorable Matrix Constitutions for Controllable Transdermal Drug Delivery. Macromolecular Materials and Engineering, 2018, 303, 1800233.	3.6	31
95	Blood sampling using microneedles as a minimally invasive platform for biomedical diagnostics. Applied Materials Today, 2018, 13, 144-157.	4.3	41
96	Light-activatable Chlorin e6 (Ce6)-imbedded erythrocyte membrane vesicles camouflaged Prussian blue nanoparticles for synergistic photothermal and photodynamic therapies of cancer. Biomaterials Science, 2018, 6, 2881-2895.	5.4	56
97	A new red fluorophore with aggregation enhanced emission by an unexpected "One-step―protocol. RSC Advances, 2018, 8, 18327-18333.	3.6	9
98	Irinotecan delivery by unimolecular micelles composed of reduction-responsive star-like polymeric prodrug with high drug loading for enhanced cancer therapy. Colloids and Surfaces B: Biointerfaces, 2018, 170, 488-496.	5.0	16
99	Methotrexate-based amphiphilic prodrug nanoaggregates for co-administration of multiple therapeutics and synergistic cancer therapy. Acta Biomaterialia, 2018, 77, 228-239.	8.3	41
100	A paper-based photothermal array using Parafilm to analyze hyperthermia response of tumour cells under local gradient temperature. Biomedical Microdevices, 2018, 20, 68.	2.8	5
101	Improving the carrier stability and drug loading of unimolecular micelle-based nanotherapeutics for acid-activated drug delivery and enhanced antitumor therapy. Journal of Materials Chemistry B, 2018, 6, 5549-5561.	5.8	10
102	Green Fabrication of Ovalbumin Nanoparticles as Natural Polyphenol Carriers for Ulcerative Colitis Therapy. ACS Sustainable Chemistry and Engineering, 2018, 6, 12658-12667.	6.7	57
103	Rapidly cell-penetrating and reductive milieu-responsive nanoaggregates assembled from an amphiphilic folate-camptothecin prodrug for enhanced drug delivery and controlled release. Biomaterials Science, 2017, 5, 444-454.	5.4	43
104	Orally Targeted Delivery of Tripeptide KPV via Hyaluronic Acid-Functionalized Nanoparticles Efficiently Alleviates Ulcerative Colitis. Molecular Therapy, 2017, 25, 1628-1640.	8.2	138
105	Organobase-catalyzed [1,2]-Brook rearrangement of silyl glyoxylates. Organic and Biomolecular Chemistry, 2017, 15, 1418-1425.	2.8	12
106	Gemcitabine–camptothecin conjugates: a hybrid prodrug for controlled drug release and synergistic therapeutics. Biomaterials Science, 2017, 5, 1889-1897.	5.4	43
107	Multifunctional silica nanoparticles as a promising theranostic platform for biomedical applications. Materials Chemistry Frontiers, 2017, 1, 1257-1272.	5.9	85
108	pH-responsive polymeric micelles based on poly(ethyleneglycol)-b-poly(2-(diisopropylamino) ethyl) Tj ETQq0 0 0	rgBT /Ovei 9.4	lock 10 Tf 50 41

Colloid and Interface Science, 2017, 490, 511-519.

#	Article	IF	CITATIONS
109	Acid-Activatable Theranostic Unimolecular Micelles Composed of Amphiphilic Star-like Polymeric Prodrug with High Drug Loading for Enhanced Cancer Therapy. Molecular Pharmaceutics, 2017, 14, 4032-4041.	4.6	33
110	PEGylated polydopamine-coated magnetic nanoparticles for combined targeted chemotherapy and photothermal ablation of tumour cells. Colloids and Surfaces B: Biointerfaces, 2017, 160, 11-21.	5.0	51
111	Surface Modification of Poly(dimethylsiloxane) with Polydopamine and Hyaluronic Acid To Enhance Hemocompatibility for Potential Applications in Medical Implants or Devices. ACS Applied Materials & Interfaces, 2017, 9, 33632-33644.	8.0	85
112	Highly cell-penetrating and ultra-pH-responsive nanoplatform for controlled drug release and enhanced tumor therapy. Colloids and Surfaces B: Biointerfaces, 2017, 159, 484-492.	5.0	9
113	pH-Responsive unimolecular micelles based on amphiphilic star-like copolymers with high drug loading for effective drug delivery and cellular imaging. Journal of Materials Chemistry B, 2017, 5, 6847-6859.	5.8	44
114	iRGD-functionalized PEGylated nanoparticles for enhanced colon tumor accumulation and targeted drug delivery. Nanomedicine, 2017, 12, 1991-2006.	3.3	27
115	Disassembly of amphiphilic small molecular prodrug with fluorescence switch induced by pH and folic acid receptors for targeted delivery and controlled release. Colloids and Surfaces B: Biointerfaces, 2017, 150, 50-58.	5.0	32
116	Isolation and retrieval of circulating tumor cells on a microchip with double parallel layers of herringbone structure. Microfluidics and Nanofluidics, 2016, 20, 1.	2.2	8
117	Functional magnetic Prussian blue nanoparticles for enhanced gene transfection and photothermal ablation of tumor cells. Journal of Materials Chemistry B, 2016, 4, 4717-4725.	5.8	22
118	Hydrophobic-Sheath Segregated Macromolecular Fluorophores: Colloidal Nanoparticles of Polycaprolactone-Grafted Conjugated Polymers with Bright Far-Red/Near-Infrared Emission for Biological Imaging. Biomacromolecules, 2016, 17, 1673-1683.	5.4	46
119	Mesoporous silica nanoparticles combining Au particles as glutathione and pH dual-sensitive nanocarriers for doxorubicin. Materials Science and Engineering C, 2016, 59, 258-264.	7.3	28
120	Glutathione- and pH-responsive nonporous silica prodrug nanoparticles for controlled release and cancer therapy. Nanoscale, 2015, 7, 5859-5868.	5.6	124
121	Glutathione-Responsive Polymeric Micelles Formed by a Biodegradable Amphiphilic Triblock Copolymer for Anticancer Drug Delivery and Controlled Release. ACS Biomaterials Science and Engineering, 2015, 1, 585-592.	5.2	78
122	Unimolecular micelles of amphiphilic cyclodextrin-core star-like block copolymers for anticancer drug delivery. Chemical Communications, 2015, 51, 15768-15771.	4.1	102
123	Preparation and Characterization of an Amphipathic Magnetic Nanosphere. Journal of Analytical Methods in Chemistry, 2014, 2014, 1-6.	1.6	3
124	Preparation of a Camptothecin Prodrug with Glutathioneâ€Responsive Disulfide Linker for Anticancer Drug Delivery. Chemistry - an Asian Journal, 2014, 9, 199-205.	3.3	62
125	A novel nanoassembled doxorubicin prodrug with a high drug loading for anticancer drug delivery. Journal of Materials Chemistry B, 2014, 2, 3433-3437.	5.8	39
126	Fabrication of Single-Hole Glutathione-Responsive Degradable Hollow Silica Nanoparticles for Drug Delivery. ACS Applied Materials & Interfaces, 2014, 6, 12600-12608.	8.0	70

IF # ARTICLE CITATIONS A new strategy to prepare glutathione responsive silica nanoparticles. RSC Advances, 2013, 3, 17700. 19 Development of hyperbranched polymers with non-covalent interactions for extraction and 128 5.4 28 determination of aflatoxins in cereal samples. Analytica Chimica Acta, 2013, 797, 40-49. Preparation and drug-delivery properties of hollow YVO<sub>4</sub>:Ln<sup>3+</sup>and mesoporous YVO<sub>4</sub>:Ln<sup>3+</sup>@nSiO<sub>2</sub>@mSiO<sub>2</sub>(Ln = Eu, Yb,) Tj ETQ6181 0.784314 rgB 129 Photoluminescent Silicon Nanocrystal-Based Multifunctional Carrier for pH-Regulated Drug 130 8.0 54 Delivery. ACS Applied Materials & amp; Interfaces, 2012, 4, 3424-3431. Carbon nanoparticles from corn stalk soot and its novel application as stationary phase of hydrophilic interaction chromatography and per aqueous liquid chromatography. Analytica Chimica 5.4 Ácta, 2012, 726, 102-108. Functionalized periodic mesoporous organosilicas for selective adsorption of proteins. Applied Surface Science, 2012, 258, 7126-7134. 132 6.1 27 Glycopolypeptide-encapsulated Mn-doped ZnS quantum dots for drug delivery: Fabrication, characterization, and in vitro assessment. Colloids and Surfaces B: Biointerfaces, 2011, 88, 51-57. Preparation and Evaluation of Poly-I-Lysine Stationary Phase for Hydrophilic 134 1.341 Interaction/Reversed-Phase Mixed-Mode Chromatography. Chromatographia, 2011, 74, 523-530. Synthesis and characterization of Fe3O4@SiO2@poly-l-alanine, peptide brushâ€"magnetic microspheres through NCA chemistry for drug delivery and enrichment of BSA. Colloids and Surfaces B: Biointerfaces, 2010, 81, 503-507. 5.0 39 Preparation and characterization of L-Leucine-modified amphiprotic bifunctional mesoporous SBA-15 136 6.1 24 molecular sieve as a drug carrier for ribavirin. Applied Surface Science, 2010, 256, 3160-3165. Preparation of magnetic molecularly imprinted polymer for rapid determination of bisphenol A in 3.7 environmental water and milk samples. Analytical and Bioanalytical Chemistry, 2009, 395, 1125-1133. Oxidized Multiwalled Carbon Nanotubes as an SPME Fiber Coating for Rapid LC–UV Analysis of 138 1.3 31

Benzimidazole Fungicides in Water. Chromatographia, 2009, 70, 753-759.

**ZHIGANG XU**